scientific reports

Check for updates

OPEN

Experimental maturation of pine resin in sediment to investigate the formation of synthetic copal and amber

Evan T. Saitta[1]✉ & Thomas G. Kaye[2]

Experimentally simulating fossil resin formation would improve our understanding of copal/amber and could simulate the diagenesis of resin inclusions. Resin from living *Pinus* underwent sediment-encased maturation under various temperature and pressure conditions. Light microscopy suggests that matured resin dries, possibly hardens, and darkens into a brittle, yellow–orange–brown translucent mass with increased luster, exhibiting flow lines, birefringence, conchoidal fracturing, and air pockets typical of copal/amber. Leached components were observed in the sediment. Infrared spectroscopy suggests that matured resins have spectra consistent with those of fossil resins and may exhibit similar differences from fresh resin—possibly decreased relative intensity of C=O stretching at ~ 1700 cm^{-1}. Results suggest desiccation and volatile/labile component loss, alongside potential polymerization/cross-linking of stable components into a macromolecule (although we discuss the challenge of 'Class V ambers'). 'Synthetic copal/amber' is amenable to destructive analyses and would guide studies of fossil resin inclusions in informed, predictable, and targeted manners to limit loss of rare specimens. With novel experimental methods involving fresh resin and utilizing sediment porosity, our work expands upon insights from commercial autoclaving of natural subfossil copal/fossil amber used to alter their physical properties. Considering the broad success of sediment-encased maturation to simulate carbonaceous compression fossils and ancient resins, we predict that experimental taphonomy will elucidate the fossilization potential of diverse plant biomolecules and even plant secondary metabolites related to herbivory, flavor, and pharmacology.

Paleontology has greatly expanded in recent decades to become multi-disciplinary and even experimental, due in part to the complexity of the interacting biological, physical, and chemical processes of taphonomy during fossilization[1]. Taphonomic experiments used to study the degradation and preservation of organismal tissues inform upon both biases in the fossil record as well as novel avenues of research using fossil biomolecules[2].

Artificial maturation applies high heat and pressure to various tissue types under laboratory timescales in order to simulate long-term diagenesis where a fossil is buried for millions of years. Analogous to pressure cooking, artificial maturation uses elevated pressures to allow for higher temperatures while maintaining reactions comparable to natural conditions (e.g., by preventing water from boiling, aqueous chemistry is maintained). Thus, artificial maturation induces greater alteration to samples over shorter timeframes than would be possible at lower pressures and temperatures, making artificial maturation a staple experimental approach for studying the formation of ancient organic material by numerous researchers for decades e.g.,[2–24]. Recently, we[25,26] have shown that artificial maturation within compacted sediment yields organic residues that are in many ways microscopically and chemically similar to 'carbonaceous compression fossils' (see definition in[27]). This similarity is due to sediment pores allowing breakdown products from volatile or labile tissue components to escape, while retaining stable components[25]. Sediment-encased maturation thereby improves upon standard maturation by allowing for a more naturalistic open system. Such simulations help us to construct models of diagenesis, thereby guiding our study of fossil taphonomy and the hunt for fossil biomolecules.

Of the various modes of preservation observed in the fossil record, amber and copal inclusions are among the most spectacular but have only in recent decades been studied extensively with an eye towards their molecular taphonomy[28,29]. The preservation of inclusions in subfossil copal and fossil amber is of great research interest, but is often limited to non-destructive chemical analyses, such as Raman spectroscopy, nuclear magnetic resonance spectroscopy, X-ray diffraction, or infrared spectroscopy e.g.,[30–44], due to curatorial concerns and the rarity of

[1]Life Sciences Section, Negaunee Integrative Research Center, Field Museum, Chicago, IL, USA. [2]Foundation for Scientific Advancement, Sierra Vista, AZ, USA. ✉email: evansaitta@gmail.com

certain types of inclusions (e.g., vertebrates[45] or ammonites[46]). Reports of endogenous biomolecules include the hardy biopolymers of insect chitin[47] and fungal melanin[48]. Other reports of biomolecules are sometimes found to have mixed results, such as feather amino acids ([49], but see[50]) or to be outright controversial, such as DNA ([51], but see[52]). Many amber inclusions are simply void spaces within the organic matrix of this fossil resin[53]. The ability to simulate amber formation in the lab, therefore, would be extremely practical in studying both amber formation and inclusion preservation. Not only would conditions be controlled in the laboratory and replicable, but the samples would also be amenable to highly destructive chemical analysis.

Sub-fossil copal and fossil amber generally represent various degrees of desiccation and volatile loss in plant resins (e.g., monoterpenoids, sesquiterpenoids, water), as well as polymerization/cross-linking of their stable organic compounds (e.g., diterpenoids and triterpenoids)[54–56]. In other words, the starting oleoresin contains essential oils that are volatilized, while the resin component remains and can polymerize/cross-link, processes that can be accelerated under the heat and pressure of diagenesis. Therefore, tree resin is a logical tissue type on which to perform sediment-encase maturation experiments. These ancient resins are heterogenous with fractions of varying solubility in organic solvents[57]. In addition to polymerization/cross-linking with increased maturity, these ancient resins can also undergo isomerization and cyclization[58]. Typically, amber has a refractive index of ~ 1.5–1.6, Moh's hardness of ~ 2.0–2.5, and a melting point of ~ 250–300 °C[59].

Chromatography has revealed diverse terpene biomarkers that correlate to taxonomy of the source resin[44]. Fossil resins can therefore be diverse in their composition, depending on their source plant. For example, Eocene Baltic amber, also known as 'succinite', comes from conifers, but there is debate as to the number and identify of the precise source species. Wolfe et al.[60] used Fourier-transform infrared micro-spectroscopy to conclude that Baltic amber is more likely to have derived from the conifer family Sciadopityaceae than from either Cupressaceae or Pinaceae conifer families, as had been previously proposed. Although amber is often described as resulting from polymerization, some believe that amber is better described as a 'macromolecule' resulting from cross-linking of diterpenoids and triterpenoids with some of the pore spaces filled with residual molecules of smaller monoterpenoids and sesquiterpenoids (sometimes physically or chemically bonded to the macromolecule) to form a 'supramolecule'[61]. Under this definition, the amber is not simply a repeating chain of monomers making up a typical 'polymer'.

The current state of the art on altering amber is driven in large part by the commercial gemstone trade, which uses autoclaves to expose naturally occurring subfossil copal or fossil amber to elevated heat (e.g., 90–180 °C) at either atmospheric or relatively low (e.g., 25–35 bar) pressure[62]. Doing so matures copal and amber in order to induce changes to their optical properties (e.g., darkening or color/fluorescence change, such as commercially altered 'green amber' from autoclaving[33]). Other studies have experimentally simulated aging of copal and amber to mimic weathering or maturation e.g.,[63,64], but these also typically start off with natural copal or amber samples. Experimentation with modern, fresh resins that does not comprise of photodegradation by light, has involved either decaying inclusions at room temperature and pressure[65] or heating samples without elevated pressure[66], which although expected to induce dehydration, likely does not fully mimic the formation of natural amber.

Here, we attempt to improve upon experimental design by performing sediment-encased, high-heat, high-pressure artificial maturation[25] on freshly collected resin, rather than subfossil copal. Like a pressure cooker, temperatures and pressures exceed those experienced in natural taphonomic settings in order to more fully account for the vast amounts of time that fossil resins can degrade over. The testable prediction is that sediment pore filtration will simulate the natural formation of amber. The more volatile compounds (e.g., monoterpenoids and sesquiterpenoids, as well as water[56]) are lost to form copal, followed by potential polymerization/cross-linking of more stable compounds (e.g., diterpenoids and triterpenoids) to form actual amber[54,55], while some aromatization may also occur[40]. In this sense, the work below is more engineering of novel methodology that can then lead to highly systematic experimentation in the future. We judge the efficacy of our method through photography, digital microscopy, and attenuated total reflectance-Fourier transform infrared spectroscopy (ATR-FTIR).

A note on resin IR

Given our methodology, it is worth introducing the impact that resin maturation has on the infrared spectra of this organic matrix, as well as the characteristic IR peaks that have previously been ascribed to fresh resin, copal, and amber. We present here a general summary of past IR interpretations, while acknowledging that diverse amber sources (i.e., taxonomy) and precise methodological conditions can complicate such interpretations. Even intraspecific variation can appear in IR spectra of different modern resins e.g.,[67,68]. Differences between and among fresh and fossil resins are often subtle. We summarize the previously observed spectra of natural and experimental resins and report the peak assignments designated by those studies, noting that such assignments are not necessarily certain.

Although the species of plant impacts its resin's spectra[31], prior research has shown that amber and fresh resin often have broadly similar IR spectra[62]. Liang et al.[40] showed that amber has a reduction of relative peak intensity at ~ 1700 cm^{-1} (C=O stretching from carbonyl and carboxyl) compared to fresh resin, but caution should be exhibited if attempting to interpret this single band in isolation when judging resin age or thermal alteration. There are also possible signs of aromatization with a peak at 1605 cm^{-1} (aromatic C=C stretching) appearing in amber[40]. Liang et al.[40] found that both fresh resin and amber also have symmetric stretching vibrations (1370–1480 and 2800–3000 cm^{-1}), phenolic OH (1265 cm^{-1}, whose detection can vary depending on methodological conditions), C–O–C stretching (1247 cm^{-1}), and asymmetric C–O–C stretching (1030 cm^{-1}).

Even experimentally pressure- and heat-treated subfossil resins (i.e., copal) were observed by Zheng et al.[62] to show only minor changes in their IR spectra, although there was a weakening of the relative peak intensity at ~ 3078 (C–H stretching of exocyclic C=CH_2), 1642 (exocyclic non-conjugated C=C stretching), and 888 (out-

of-plane C–H bending of exocyclic methylene) cm^{-1} with more intensive treatment. Also observed was a shift from C = O related to esters from a peak position ~ 1697 cm^{-1} to higher values up to 1727 cm^{-1}[62]. Zheng et al.[62] suggested these results indicate the breaking of exocyclic unsaturated bonds as polymerization/cross-linking increases (i.e., saturation increases) and reduced concentrations of labdanoid diterpenes monomers during polymerization/cross-linking. Labdanoid diterpenes are responsible for the majority of natural ancient resins[69].

Likewise, it has been suggested by García-Vallès et al.[43] that, compared to more mature Eocene fossil Baltic amber, subfossil Congo copal (estimated Pleistocene to recent age[70]) contains more intense FTIR peaks at 3095 (C–H stretching in exocyclic $C=CH_2$), 1643 (C=C stretching in $RCH=CH_2$, $RR'C=CH_2$ unsaturated compounds), 1265 (C–O stretching), and 887 (C–H bending) cm^{-1}. Like the Congo copal, the Baltic amber still showed FTIR peaks at 3328 (O–H stretching from water), 2926 (C–H stretching from methyl and methylene groups) and 2852 (saturated bands), 1735 (C=O stretching), 1645 (C=C stretching), 1457 (CH_2 bending), 1375 (CH_3 bending), a wide absorption shoulder from 1255 to 1156 ('Baltic shoulder' from C–O stretching of esters, alcohols, and carboxylic acids), 1156 (C–O–O stretching), 992 (C–H bending), and 887 (C–O bending) cm^{-1}[43].

Another study of Baltic amber by Wagner-Wysiecka[38] using mid-infrared spectroscopy also identified the following peaks: O–H stretching, C–H stretching from unsaturated bonds (3080 cm^{-1}), C–H stretching from methyl and methylene groups, saturated bonds (2940–2960 cm^{-1} and 2930, 2870, 2850 cm^{-1}), C=O stretching from esters (1736 cm^{-1}) and carboxylic acids (1700 cm^{-1}), C=C stretching from unsaturated $RCH=CH_2$, $RR'C=CH_2$ (1642 cm^{-1}), C–H bending from methyl and methylene (1455, 1375 cm^{-1}), C–O stretching from esters, alcohols, and carboxylic acids of the 'Baltic shoulder' (1260–1160 cm^{-1}), C–O–H stretching from alcohols (1020 cm^{-1}), C–H out-of-plane vibration in $RCH=CH_2$ (980 cm^{-1}), and C–H out-of-plane vibration in $R_2C=CH_2$ (888 cm^{-1}). Note that the precise assignment of bands 887 and 888 cm^{-1} can differ between studies.

Institutional abbreviations

CBG: Chicago Botanic Garden, Glencoe, IL, USA;
FSA: Foundation for Scientific Advancement, Sierra Vista, AZ, USA;
MAI UG: Museum of Amber Inclusions, University of Gdańsk, Gdańsk, Poland.

Materials & methods

Samples

Pinus is one of the easiest trees to sample resin from in North America, where we are based. Furthermore, Saitta et al.[25] had presented some early results of sediment-encased maturation of pine resin (which was scraped off the bark of a living Aleppo Pine [*Pinus halepensis*] growing at FSA) using an older design of the maturation equipment, meaning that continued focus on *Pinus* here allowed for comparison to those initial results.

New samples were obtained and then treated in this study with improved sediment-encased maturation equipment at the University of Chicago (based on equipment described in[26]). Samples for this thermal maturation were scraped off the bark of three trees at the CBG (Table 1). One Mountain Pine (*Pinus mugo*) and two Scots Pines (*Pinus sylvestris*). One *P. sylvestris* tree had sticky, moist, fragrant resin (i.e., the oleoresin presumably contained higher concentrations of volatile oil of turpentine/moisture compared to rosin), while the other had relatively dryer resin – presumably as a result of longer exposure or other variable conditions (e.g., temperature, wind, sun exposure) at the tree's external surface.

Resin sample	Resin notes	Source	Maturation run	Clay	Compaction	Temperature	Pressurizing gas	Pressure	Total duration*	Run description
Sticky *P. sylvestris***	Sticky, moist, & fragrant	CBG	A	Bentonite	8 metric tons	~ 130 °C	Air	~ 159 bar for 22 h, then ~ 248 bar for 0.5 h	~ 22.5 h	Low pressure, then short period of high pressure, all while under heat
P. mugo										
Dry *P. sylvestris*	Dry									
Dry *P. sylvestris*	Dry	CBG	B	Bentonite	8.5 metric tons	~ 135 °C for 22.7 h, then cool down	Air	~ 241 bar for 24.25 h	~ 24.25 h	High pressure, which continued after cool down
Sticky *P. sylvestris*	Sticky, moist, & fragrant	CBG	C***	Bentonite	8–8.5 metric tons	~ 135–140 °C for 19.05 h, then cool down to ~ 30 °C, then ~ 145–150 °C for 24.08 h	Air	~ 241 bar during first heating, then vented to ~ 172 bar before second heating, then brought back to ~ 241 bar during second heating	~ 41.13 h	Double heating at high temperature, high pressure
P. mugo										
Dry*P. sylvestris*	Dry									
Sticky *P. sylvestris*	Sticky, moist, & fragrant									
P. mugo										
Dry *P. sylvestris*	Dry									
Fresh Resin	Untreated, freshly collected	FSA	NA	NA	NA	NA	NA	NA	NA	NA

Table 1. Samples were analyzed with photography, digital light microscopy, and/or IR spectroscopy in this study, and details are provided for each maturation run. *Excluding initial pressurization to ~ 172 bar before heating, final cool down, and final depressurizing. **Clay tablet unopened & sample not analyzed to preserve surface leakage on it from Dry *P. sylvestris* in same run. ***Thermocouple temperature data logged.

After digital light microscopy, the ATR-FTIR spectra of these samples were compared to fresh resin scraped from the surface of an Aleppo Pine growing at the FSA. FTIR spectra from Szwedo & Stroiński[37] of natural fossil Baltic amber (Gulf of Gdańsk, secondary deposit) specimen MAI UG 508,762 from the Eocene[71] was also compared to our experimental maturation results.

Sediment-encased maturation

Maturation of samples was performed in compacted sediment using the methodology of Roy et al.[26], an updated version of Saitta et al.[25] (see supplemental material for schematic diagram). Many of the conditions were generally inspired by previous maturation experiments (e.g.,[25,26]), helping to ease comparisons across studies. Therefore, we could help to control against some of the effects of compaction force, pressure, or duration by keeping them similar to those of earlier tests.

All samples were first compacted in a hydraulic press at 8–8.5 metric tons across a 13 mm diameter circular surface area of the pill press while buried in food-grade bentonite (sodium montmorillonite) from the brand Fossil Power. Compacted samples encased in sediment were then transferred to the maturation chamber to be pressurized and heated. Multiple samples (i.e., tablets of compacted sediment with a lump of resin encased inside) are loaded into the chamber for a given run so that all of those samples experience the same conditions, controlling against things such as temperature fluctuations in the room.

All maturation occurred under pressurized air, which is the most readily available gas to feed into the air compressor and follows previous studies[25,26], so it is important to note that these particular results may better simulate relatively oxic conditions during diagenesis than strictly anoxic conditions (future work could use pressurized N_2 gas). Three maturation conditions were studied. We generally ran experiments at lower temperatures than past studies and also included a multi-step heating treatment under the assumption that resin curation can occur at milder conditions than alteration of other fossil organics. For example, when the highly recalcitrant pigment melanin is treated in sediment-encased maturation, 190–225 °C yields residues comparable to carbonaceous compression fossils according to time-of-flight secondary ion mass spectrometry[26]. Table 1 describes the samples analyzed in this study that underwent each maturation run and the precise experimental conditions of each run. Prior to turning on the heat, pressure was typically first raised to ~ 172 bar.

Run A was performed at ~ 130 °C. It involved relatively low pressure (~ 159 bar) for 22 h, followed by a short period of high pressure (~ 248 bar) for 30 min. Both low- and high-pressure periods occurred during heating.

Run B was performed at ~ 135 °C for 22.7 h and then allowed to cool to room temperature. Air was kept at a relatively high pressure (~ 241 bar) throughout heating and even after the heat was shut off, for a total of 24.25 h.

Run C occurred after the lab's acquisition of a Supco SL500TC Thermocouple Temperature Data Logger, allowing for more precise recording of temperature throughout the duration of the experiment. This run involved two pulses of heating. The first heating was ~ 135–140 °C for 19.05 h, followed by a cool down to about ~ 30 °C, then a second heating at a slightly higher temperature of ~ 145–150 °C. Air pressure was at ~ 241 bar during the first heating, followed by venting to ~ 172 bar before the second heating, and then brought back to ~ 241 bar during the second heating. Run C included two samples for each of the three resin types.

After maturation was performed, the equipment was allowed to cool down (if not already cool) to roughly room temperature, before slowly depressurizing and retrieving the samples from the chamber.

Light microscopy & photography

The clay tablet containing the dry *P. sylvestris* resin from run A split unintentionally at some point before removal from the chamber but was examined using digital light microscopy. The digital microscope was a Dino-Lite Edge AM73915MZTL (10X ~ 140X; 5.0MP; USB 3.0). The brittle nature of matured resin may make such damage more difficult to avoid.

Additionally in Run A, some resin leaked during maturation that was found on the surface of another compacted clay tablet. The fluid nature of uncured resin can lead to such difficulties. We think this most likely derives from the same split tablet containing the Run A dry *P. sylvestris* resin (it is possible it comes from Run A *P. mugo* resin instead), and this surface leakage was also studied with digital microscopy. The compacted clay tablet bearing this surface leakage (i.e., tablet containing Run A sticky *P. sylvestris* resin) was not opened to preserve the unique observations from the surface leakage atop of it.

Finally, the dry *P. sylvestris* resin from Run B was prepared by hand using a pin vise and imaged using digital microscopy. Run A *P. mugo* resin was split open using a razor blade and photographed using an iPhone 14 given its poor preservation. Beyond microscopy, this iPhone 14 camera was also used to obtain photographs, especially prior to maturation.

ATR-FTIR spectroscopy

Owing to their more precise temperature logging, samples from Run C (*P. mugo*, dry *P. sylvestris*, and sticky *P. sylvestris*) were extensively examined via ATR-FTIR spectroscopy. Their spectra were compared to the figured Run A dry *P. sylvestris* resin (excluding its possible leakage), Run A *P. mugo* resin, Run B dry *P. sylvestris*, fresh Aleppo Pine resin from outside of the FSA (Sierra Vista, AZ, USA), and a previously published ATR-FTIR spectrum from natural Eocene fossil Baltic amber MAI UG 508,762[37]. Note that the experimentally matured resins were analyzed with ATR while compacted in clay sediment, which possibly added some noise to the results due to heterogenous composition.

ATR-FTIR spectroscopy was performed at the Foundation for Scientific Advancement lab (Sierra Vista, Arizona, USA) on a Nicolet 510P FTIR, with Thermo Scientific OMNIC spectra software. For each sample, we used 50 scans at 16 cm^{-1} resolution, 0.4178 cm/s velocity. All spectra were background subtracted at the same exposure time as the samples. Finally, the spectral data files obtained were analyzed using Spectragryph v1.2.16.1 software for presentation here.

Results

Light microscopy & photography

Resin that has been artificially matured through sediment-encased maturation are not only altered in their appearance and physical properties, but they also gain many features typical of true amber and copal. The fresh, modern pine resin starts off as opaque, pale/off-white, and soft/pliable. Sometimes fresh, modern pine resin is even sticky, moist, and fragrant (excepting the dryer *P. sylvestris* resin) (Figs. 1, 2, 3). However, maturation alters

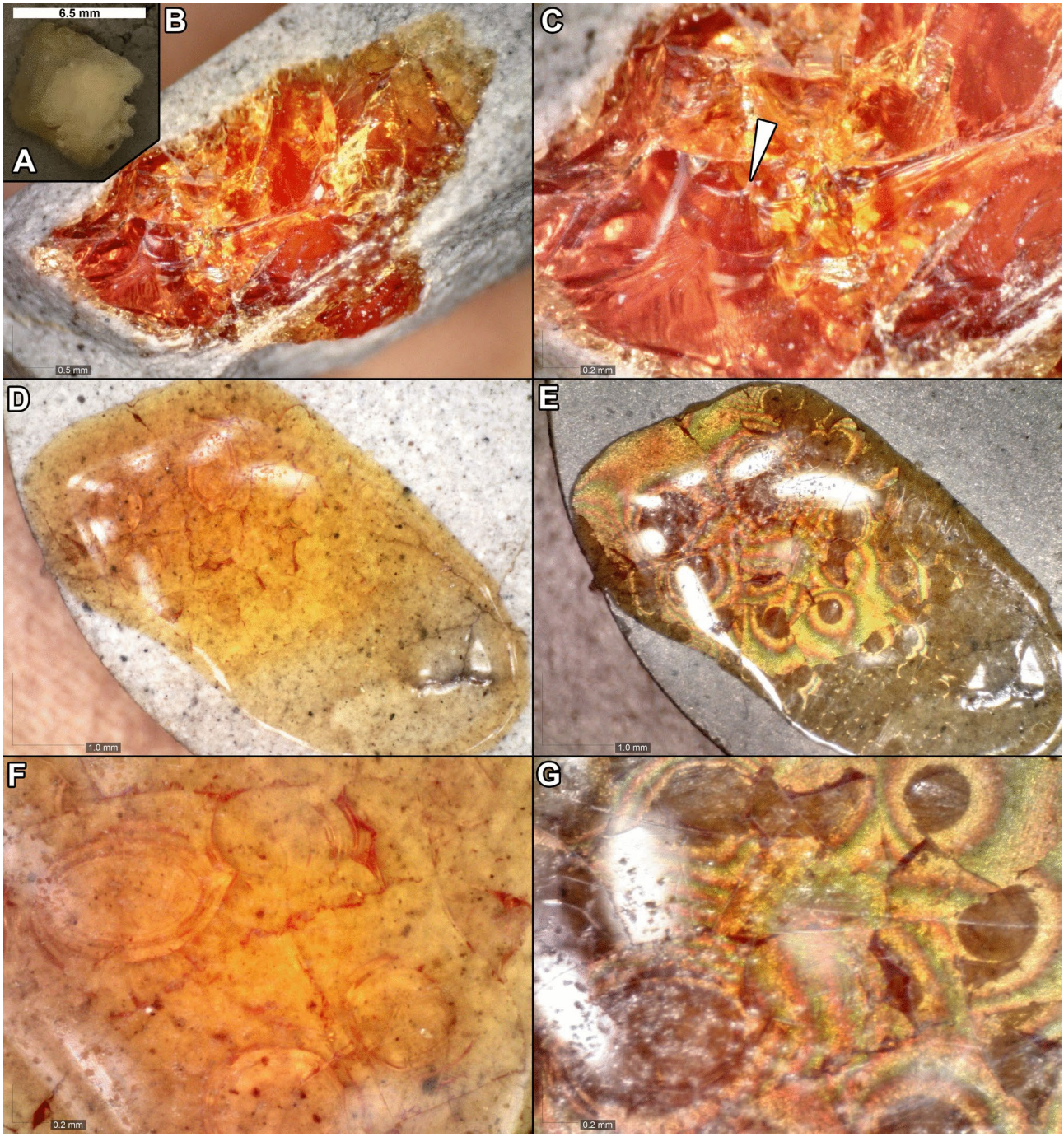

Fig. 1. Run A results from dry *P. sylvestris* resin. (**A**) Resin before maturation, showing pale off-white coloration and opacity. (**B**) Split tablet's broken edge, showing darkening, translucence, and brittleness. (**C**) Close up of bottom left region of (**A**) showing conchoidal fracturing (arrow). (**D**–**G**) Resin we suspect likely leaked from this sample during maturation onto the surface of another, unopened tablet. Yellow, translucent, birefringent surface leakage showing prominent luster in (**D**) parallel polarization and (**E**) cross polarization settings of the microscope. Close up of the top left region of (**D**–**E**) showing circular flow lines and preference in (**F**) parallel polarization and (**G**) cross polarization.

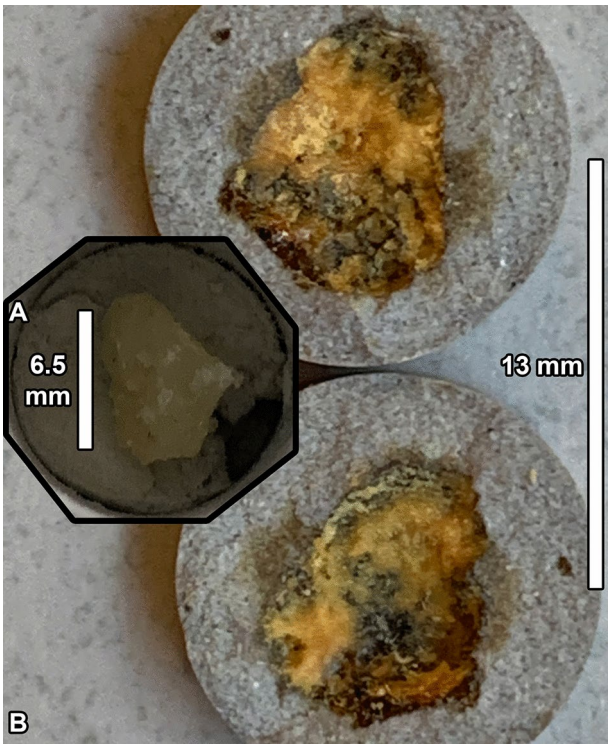

Fig. 2. Run A results from the *P. mugo* resin. (**A**) Resin before maturation, showing light coloration and opacity. (**B**) Part and counterpart after maturation, showing loss of mass/volume to produce a large cavity, as well as poorer preservation than in Fig. 1.

these resins, as seen in this study (Figs. 1, 2, 3) as well as in the supplemental results of Saitta et al.[25] (Fig. 4). Novel features that are consistent with at least copal and especially amber or their formation include:

1) Darkened coloration, ranging from yellow to orange to brown (Figs. 1, 2, 3, 4)
2) Increased dryness/desiccation/dehydration (Figs. 1, 2, 3, 4)
3) Increased luster (Figs. 1, 3 and 4)
4) Increased translucence (Figs. 1, 3 and 4)
5) Increased brittleness and tendency to crumble/break (e.g., as seen in the unintentionally split tablet in Fig. 1)
6) Possibly increased hardness compared to the pliable fresh resin, as qualitatively judged by contact with handheld preparation tools (i.e., pin vise) (Figs. 1, 2, 3, 4); note that this change was not quantified on the Mohs scale and so should be considered tentatively.
7) Appearance of conchoidal fracturing (Fig. 1)
8) Appearance of flow lines (Fig. 1)
9) Appearance of birefringence under cross polarization (Fig. 1)
10) Volume/mass loss and air pocket formation (Figs. 2, 3, 4)
11) Loss of volatile/labile components into the surrounding sediment matrix, as shown in Saitta et al.[25] (Fig. 4).

The Run A *P. mugo* resin (Fig. 2) did not survive maturation nearly as well as the Run A dry *P. sylvestris* resin (or even Run B dry *P. sylvestris* resin, see below) in terms of total recovered material. This shows that starting composition of the resin can impact its preservation potential through maturation. In particular, the dry *P. sylvestris* resin survives quite well through maturation. Perhaps this is due to its desiccation/volatile loss while on the bark of the tree prior to maturation, which would be consistent with the formation of copal prior to significant polymerization/cross-linking, or this is due to differences in starting composition of the resin between the species.

Despite using an earlier design for the sediment-encased maturation equipment than that used here, the results from Saitta et al.[25] are consistent with the new results. Those prior runs were at much higher temperature and pressure than Runs A, B, or C. It is perhaps unsurprising that the preservation of this earlier sample is similar to the Run A *P. mugo* resin, where it too is largely a void space left behind in the sediment, with preserved hardened, darkened resin only at the edges of this cavity. See Fig. 4 for details of the precise maturation conditions of the Saitta et al.[25] Aleppo Pine resin sample.

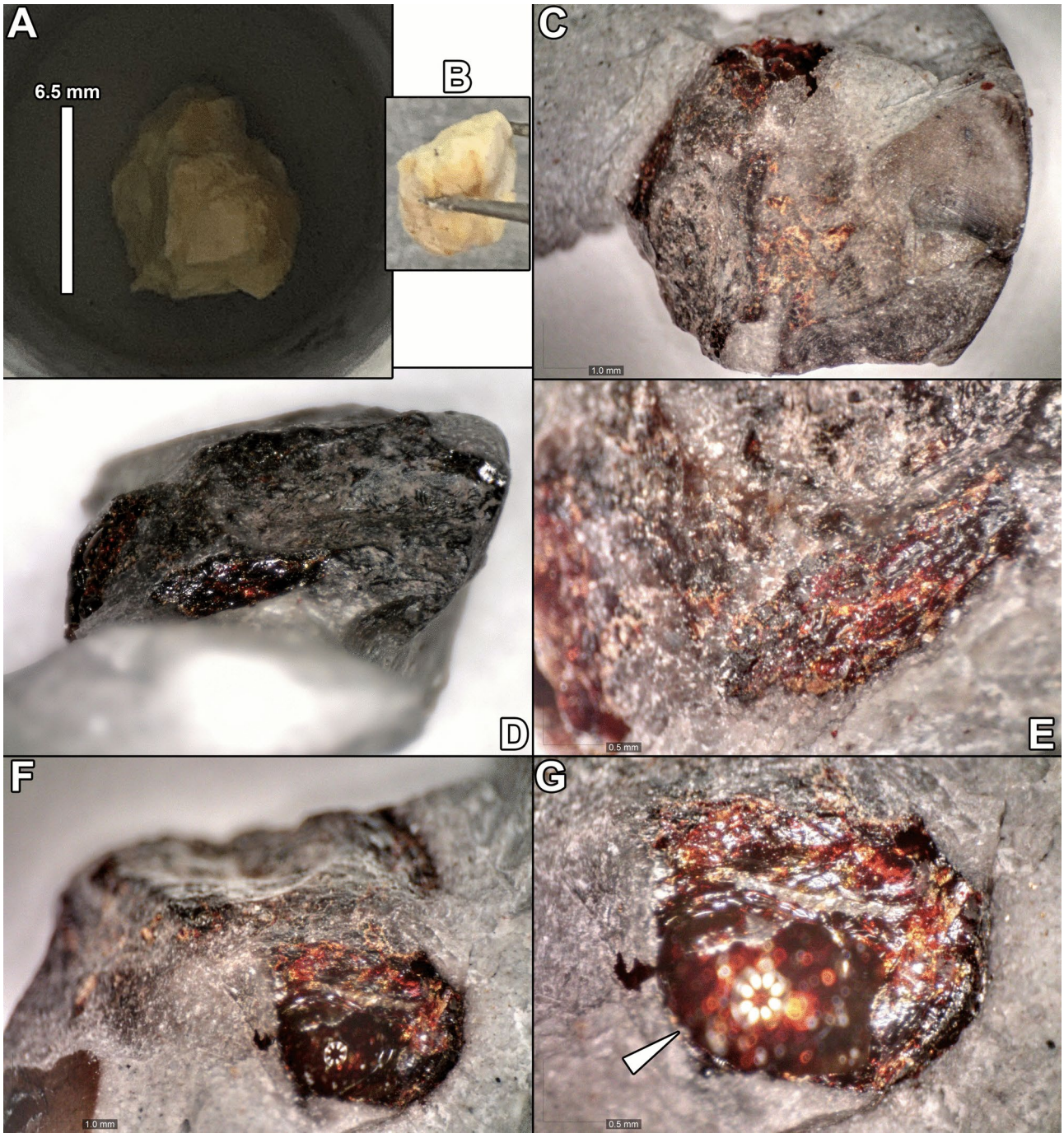

Fig. 3. Run B results from dry *P. sylvestris* resin. (**A**–**B**) Resin before maturation, showing light coloration and opacity. Top (**C**) and side (**D**) view of hand-prepared tablet after maturation, showing darkened color and translucence. (**E**) Close up of the side view in (**D**) showing surface texture. (**F**) Front view and close up (**G**) showing large air pocket produced (arrow) and prominent luster.

ATR-FTIR spectroscopy

Although susceptible to difficult background correction (e.g., from possible air pockets and reduced contact with the resin), the spectra are all generally consistent with spectra from fossil resins described above and often bear the characteristic high-absorbance peaks, as seen in Fig. 5. Given the uncertainties often present in IR peak assignment, we therefore attempted to analyze our spectra extremely conservatively.

The matured resins tend to show alterations from fresh resin as might expected from fossil resins. Namely, we observed a decrease in the relative intensity of the C=O stretching peak around ~ 1700 cm^{-1} that might be possible evidence of increased maturation if these putative C=O bonds represent exocyclic carbonyl and carboxyl groups. Using the interpretations from prior studies, these bonds would derive from labdanoid

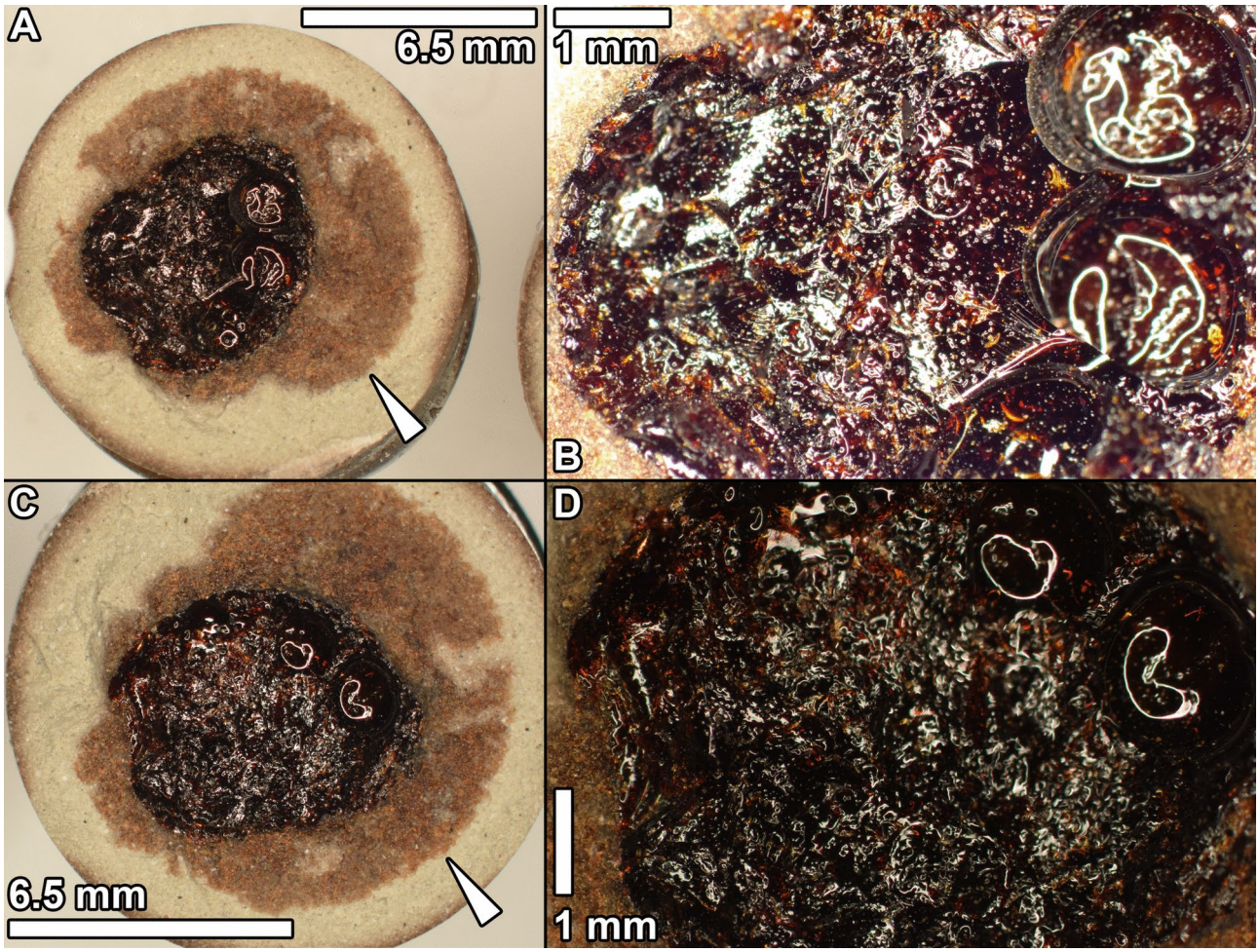

Fig. 4. Previous experimental results from Saitta et al.[25], using older sediment-encased maturation equipment than presented here (e.g., heat produced by placing pressurized chamber in a laboratory oven instead of by a localized, insulated heating coil around the pressurized chamber). Pine resin (scraped from living Aleppo Pine at FSA) in calcium bentonite compacted at ~ 9.1 metric tons over a 126.7 mm^2 surface area. Maturation was at ~ 250 °C and ~ 230–300 bar (pressurized air) for ~ 23 h. Part (**A**–**B**) and counterpart (**C**–**D**) of the tablet, showing darkly colored, translucent, hardened resin with a front of leaching labile material out into the sediment matrix (arrows) (**A**, **C**) and air pockets within an overall largely voided space (**B**, **D**). Images modified from supplemental material of Saitta et al.[25].

diterpene monomers whose concentrations are reduced through covalent incorporation into the macromolecular structure[40,62]. Modern pine resins from the genus *Pinus* have indeed been shown to contain various diterpenes e.g.,[72,73], including labdanoid diterpenes and those with exocyclic C=O bonds from carbonyl and carboxyl groups e.g.,[74–77]. Baltic amber forms in large part from the cross-linking of the labdanoid diterpenes communic acid and communol, which bear exocyclic C=O bonding, and also contains elevated quantities of the non-terpenoid dicarboxylic acid known as succinic acid that polymerizes to its macromolecular structure through esterification[60,78]. Bornyl acetate also bears a C=O bond and is a primary odor-producing compound from modern Pinaceae essential oils[79], meaning it is volatile and would likely be eliminated during maturation as well, which could further reduce the relative intensity of the C=O peak.

While this C=O stretching peak is relatively the most intense in fresh resin, it is not the most intense in fossil amber and in some of the matured resins here (Run B dry *P. sylvestris* resin, Run C sticky *P. sylvestris* resin, and one of the two samples for Run C dry *P. sylvestris* resin). Even when this C=O stretching peak has the highest absorbance within the matured resins, it appears to be reduced in relative intensity compared to the that of fresh resin (e.g., Run A *P. mugo* resin, one of the samples of Run C dry *P. sylvestris* resin, Run C *P. mugo* resin). Run A dry *P. sylvestris* resin and Run A *P. mugo* resin also show a slightly higher peak wavenumber for these putative C=O stretches (i.e., closer to 1700 cm^{-1}) compared to fresh resin, consistent with changes observed during experimental maturation of copal[37,62].

Given the noise in our spectra, the diminution of the major peak in fresh resin attributed to C=O bonds could be further impacted by a concurrent diminution of the relative intensity of the nearby peak from exocyclic C=C bonds (~ 1642–1645 cm^{-1}) as saturation increases during maturation through polymerization/cross-linking[43,62].

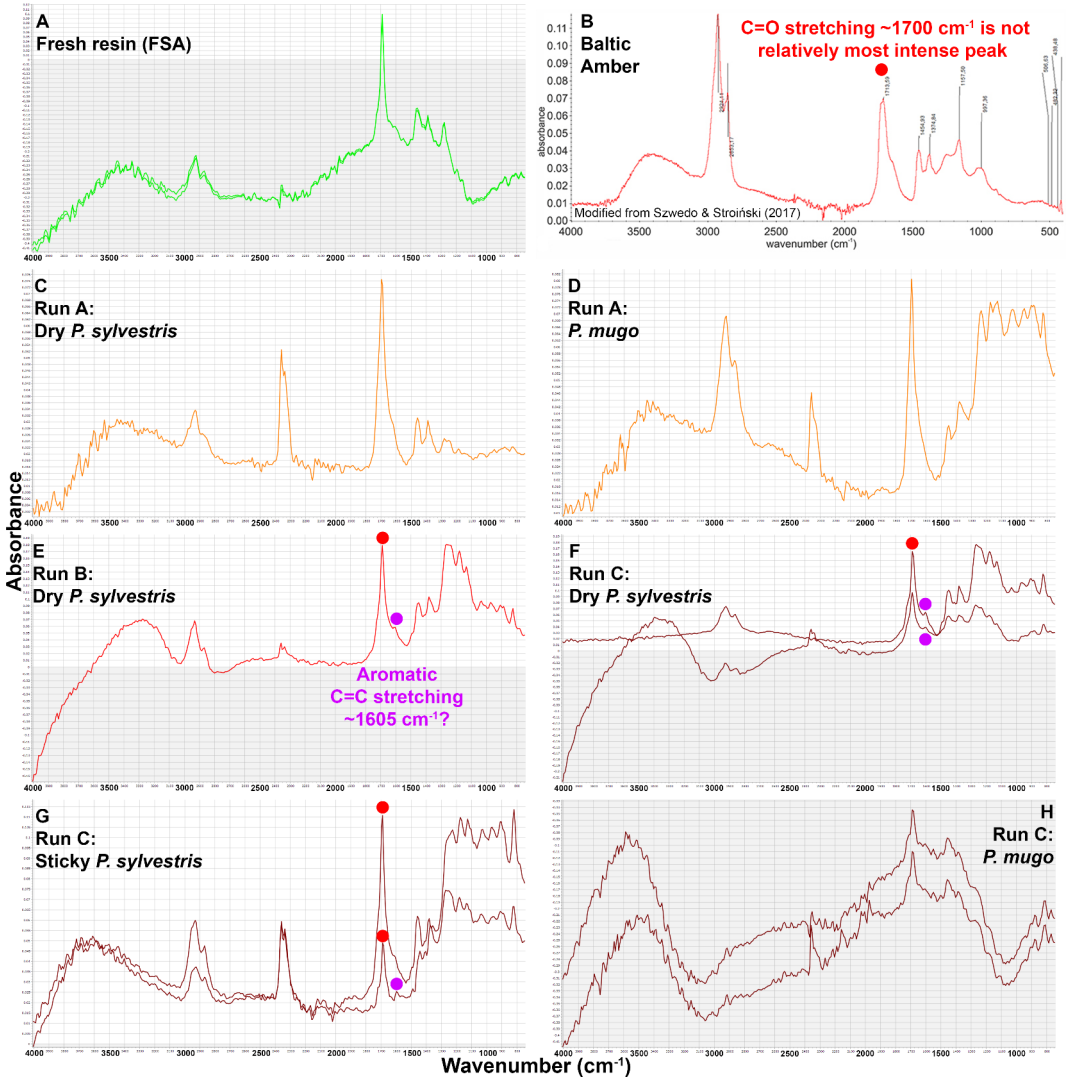

Fig. 5. ATR-FTIR spectra of fresh (**A**), fossil (**B**), and sediment-encased matured (**C**–**H**) resins. (**A**) Fresh Aleppo Pine resin from outside of the FSA (Sierra Vista, AZ, USA). Two spectra were obtained from the same sample. (**B**) Natural Eocene fossil Baltic amber MAI UG 508,762 (also ATR-FTIR and baseline corrected) modified from Szwedo & Stroiński[37] (CC BY-NC-SA 4.0). (**C**) Run A dry *P. sylvestris* resin (excluding its possible leakage). (**D**) Run A *P. mugo* resin. (**E**) Run B dry *P. sylvestris* resin. (**F**–**H**) Run C contained two samples of each resin type (e.g., two separate pieces of *P. mugo* resin were compacted separately into two separate clay tablets and then matured at the same time in the maturation chamber, alongside the other Run C samples). (**F**) Run C dry *P. sylvestris* resin. (**G**) Run C sticky *P. sylvestris* resin. (**H**) Run C *P. mugo* resin. Red dots indicate ~ 1700 cm^{-1} C=O stretching peaks that are not the most intense peak relative to their spectrum, as expected as resins mature. Purple dots indicate ~ 1605 cm^{-1} peaks that might derive from aromatic C=C stretching, as possibly expected during resin maturation. Negative absorbance values (grey) in (**A**) and especially (**H**) indicate difficulties in background correction (e.g., air pockets and reduced contact with resin) and/or suboptimal measurement parameters in OMNIC software; still, many characteristic peaks can be inferred in these spectra.

Some of the matured resins might also show signs of aromatization through peaks at ~ 1605 cm^{-1} (i.e., possible aromatic C=C stretching[40]), but these peaks are small.

Discussion

Comparing artificially matured resins to copal and amber

Sediment-encased maturation has previously been shown to reasonably simulate the diagenesis of carbonaceous compression fossils at both the macroscopic and microscopic level[25]. At the chemical level, sediment-encased maturation has even been shown to simulate key diagenetic pathways (e.g., in keratin and melanin diagenesis[26]).

Here, the multiple shared optical/material and chemical properties between our experimental resins and natural copal/amber further support this methodology's utility to the study fossilization. The following lists the

observations of our experimentally matured resin and references descriptions of the same features in natural copal and, especially, amber: darkening to a yellow, orange, or brown color[80,81]; desiccation[80,82]; increased luster[80,83]; translucence[84]; brittleness[54,85]; hardening[54]; conchoidal fracturing[80,81,85–88]; flow lines[89,90]; birefringence[91]; air pockets[92–95]; and volatile/labile compound loss[55,80,96,97].

Our results therefore suggest that sediment-encased maturation can indeed simulate key pathways for the formation of copal and amber in terms of the loss of moisture, volatile, or labile components into the adjacent sediment. The loss of more volatile terpenoids and, under typical processes of amber formation, possibly the polymerization/cross-linking of remaining terpenoids is further supported by a decrease in the relative intensity of the dominant IR peak in fresh resin after maturation, as is seen in fossil resins[37,40]. This peaks possibly corresponds to C=O bonds that, under the standard amber formation model, could derive from reduction of diterpene monomers into the macromolecular structure (and possibly also influenced by a concurrent loss of exocyclic C=C bonds during saturation)[62]. If our samples are more copal-like than amber-like in their maturity, then their spectra may instead reflect elimination of volatile components more than polymerization/cross-linking. Some of the artificially matured resins may show evidence of aromatization (i.e., formation of cyclically conjugated rings)[40], but these peaks are small if they are indeed present.

The problem of class V ambers

There is a major consideration to be made for these particular experimental samples as they relate to their source species. As North American researchers, we collected *Pinus* resin due to its regional accessibility. While Baltic amber was once thought to be produced by Pinaceae pines, this has been questioned[29,60]. Baltic amber is categorized as a Class 1a amber, the most common type in the fossil record[78]. This amber forms from the polymerization/cross-linking of the labdanoid bicyclic diterpenes communic acid and communol and also contains high amounts of the non-terpenoid dicarboxylic acid known as succinic acid, such that the amber is often called 'succinite'[78].

In contrast, pine resins are said to produce Class V ambers which contain carboxylic acid-bearing tricyclic abietane/pimarane/isopimarane diterpenoids[54,98] and *n*-alkyls. Class V ambers are not considered to undergo significant polymerization/cross-linking to produce a macromolecule[99], as seen in the partly mineralized Eocene copal from the London Clay Formation known as 'copalite'[100]. As such, Class V resin is thought to be very rare in the fossil record[54,101]. There are several possible conclusions one could draw from our experiments considering this:

1) Our experiments are producing substances not found in, or at least not currently known from, nature.

   a. Compounds in modern *Pinus* that often do not polymerize/cross-link in natural depositional settings might be unnaturally induced to polymerize in our experiments, yielding products more akin to other classes of amber. For example, normally non-polymerizable abietic acid can be undergo polymerization reactions after modification, such as dimerization[102,103].
   b. Similarly, but more naturalistically, it could also be the case that Class V 'copalites' might be able to undergo some degree of polymerization/cross-linking if they experience sufficiently high diagenetic and thermal alteration. Our experiments here might thereby be simulating Class V substances of greater thermal maturity than have been currently discovered.

2) *Pinus* resin might actually contain diterpenoids or other compounds capable of polymerization/cross-linking, but the presence or concentrations of these compounds might vary taxonomically, evolutionarily, seasonally, geographically, or nutritionally (e.g., geographic and seasonal variation of terpenes, resin acids, succinic acid, and phenolics in *Pinus sylvestris* litterfall or oleoresin[104–106], nutritional variation of *Pinus nigra* terpenes and phenolics[107]). Neutral oxygen-containing diterpenoid fractions of oleoresins can greatly differ in composition between even closely related *Pinus* species[108]. *Pinus koraiensis* and *Pinus sibirica* were found to not only contain different lipophilic metabolite compositions (including labdane-type diterpenoids) from each other, but also between the needles and twigs of the same plant[109]. Resin composition as measured by ATR-FTIR, even in a single species, can vary based on the habitat and conditions (e.g., type of resin exudation stimuli or wild vs. arboretum trees)[67,68]. All of this variability could mean that the modern *Pinus* sampled here happen to be more amendable to polymerization/cross-linking than those suggested to produce Class V ambers in the fossil record.

   While abietane-type diterpenoids of pines are often considered non-polymerizable, recent research using FTIR and pyrolysis gas chromatography–mass spectrometry has suggested that such compounds are not just occluded in amber macromolecular structure, but some can indeed be bound to the structural macromolecule[110]. Furthermore, some *Pinus* trees have been reported to produce labdane-type diterpenes (e.g., '*P. eldarica*'[77], *P. nigra*[75], *P. resinosa*[111], *P. elliottii*[74], *P. monticola*[112], *P. massoniana*[113], *P. strobus*[76], *P. ponderosa*[114], *P. pumila*[115], *P. koraiensis*, *P. sibirica*[109], *P. armandii*, *P. kwangtungensis*[116], *P. pinea*[117]). In *P. massoniana*, not only have diterpenoid biosynthesis genes been identified, but there was observed a strong positive correlation between their expression and overall oleoresin yield[118]. Labdane-type diterpenoids are considered more polymerizable than abietane-type diterpenoids. Even the polymerizable labdane-type diterpenoid communic acid, a major monomer of Baltic amber, has been detected in several *Pinus* species[119], such as *trans*-communic acid in *P. thunbergii*[120], *P. luchuensis*, and *P. densiflora*[121]. *Trans*-communic acid has been shown experimentally to undergo initial polymerization around 135–170 °C when examined with IR spectroscopy[122], consistent with our experimental temperatures here.

Specific to our experimental resin sources, *Pinus mugo* has been shown to produce a labdane-type diterpenoid, which can even be esterified with succinic acid[123,124], reminiscent of Baltic amber. *Pinus sylvestris* has been shown to contain labdane-type diterpenoids in its needles and essential oils[75,119,123,125].
Although these various compounds with elevated polymerization potential have been detected in different *Pinus* species, they are not always equally expressed throughout the plant[109]. For example, Wolfe et al.[60] detected succinic acid and its esterified derivatives in the needles of *Pinus ponderosa*, but not its resin. In *Pinus thunbergii*, the labdane-type diterpenoid *trans*-communic acid was found to be more enriched in the needles than in the twigs and outer bark[120]. Still, the metabolic ability for *Pinus* to produce these compounds is nevertheless notable, and diterpenes would be expected to derive from the oleoresin throughout the pine. Under this explanation, *Pinus* resin might not be limited to producing Class V ambers *sensu stricto* as often thought. Bicyclic labdane-type diterpenoids, including communic acid, manool, and imbricatolic acid have been suggested to be present in all families of conifers[123]. Likewise, it is important to remember that although tricyclic abietane-type diterpenoids are the predominant component of *Pinus* resin[126], other conifer taxa in Podocarpaceae, Pinaceae, Phyllocladaceae, Cupressaceae, and Araucariaceae, some of which are amber-producing, also possess such non-polymerizing abietane-type diterpenoids[127]. Even Class 1a ambers, such as 'succinite' (e.g., Baltic amber) and 'glessite', have been reported to contain some tricyclic diterpenoids[100]. In this sense, it is not so much that *Pinus* cannot produce polymerized amber, but that they may not be as prone to as other taxa that are relatively more enriched in labdane-type diterpenoids.

3) Our current experimental results might be more akin to copal than to amber, whereby polymerization/cross-linking is limited and most of the observed changes were induced through desiccation and the loss of volatile/labile compounds. In this case, our experimental products might be more akin to Class V 'copalites', such as 'Highgate copalite'.

We consider explanations (2) or (3) to be more likely, and we remain agnostic until further experiments and analyses are performed. Future work should also experiment on resins more amenable to polymerization/cross-linking from Cupressaceae and Araucariaceae.

Broader potential of sediment-encased maturation: plant fossil biomolecules

The ability to naturalistically simulate the formation of copal and amber would assist not just the study of ancient resin formation, but also the study of the diagenesis and preservation of their inclusions. Sediment-encased maturation has already shown success at reasonably simulating the diagenesis of carbonaceous compression fossils[26], including leaves and other carbohydrate-based tissues (Fig. 6), such as insect cuticles[25], down to the molecular level. Now with the potential to simulate copal/amber formation, diverse taphonomic hypotheses, especially those relating to plant biomolecules, can now be more fully tested in an experimental framework.

Plant molecular fossils have become an important data source (e.g., chlorophyl and its derivatives[128], wax alkanes[129], lignin[130]), but many additional molecules exist that might provide unique paleobiological insights, such as ecological interactions. While much work has focused on structural biopolymers, pigments, and resins (i.e., the major constituents of plant tissues), many unique compounds found in lower concentrations may have reasonably high predicted thermodynamic stability through the heat and pressure of diagenesis compared to the proteinaceous components of vertebrate tissues. These compounds could include secondary metabolites relating to herbivory attraction or deterrence[131], which in turn have been utilized for societal purposes of drugs and food seasonings[132]. Although herbivorous insects can be found trapped in fossil amber[133], the rarity of amber-producing fossil beds often limits destructive analyses due to curatorial considerations. Thus, experimental approaches that 'ground truth' taphonomic hypotheses on more expendable samples become elevated in importance.

In addition to experimental simulation of carbonaceous compression fossils[25,26], sediment-encased maturation could make it possible to study biomolecular degradation of inclusions within 'synthetic copal/amber' and then use that insight to guide destructive sampling of fossil inclusions (e.g., insects consuming plant metabolites) in amber. The following questions can be experimentally verified prior to destructively sampling rare fossils: What plant biomolecules are thermally stable and therefore more likely to survive diagenesis? Can these thermally stable biomolecules be detected in experimentally matured plant residues at sufficient concentration, or might they escape into sediment pores and be lost into the surrounding environment due to their volatility? Can those stable biomolecules be detected in other organisms that consume those plants after the consumers themselves have undergone diagenesis? What analytical methods are most efficient at detecting those biomolecules in plant and insect fossils, whether they be carbonaceous compression fossils or 3D fossil resin inclusions?

For example, modern plants and insects with fossil relatives could undergo decay and maturation experiments, followed by gas or liquid chromatography-mass spectrometry (i.e., long-established methods to study fossil biomolecules) to determine which secondary metabolites might be able to preserve in fossils and under which taphonomic conditions. Such experiments reveal the likely chemical reactions that modern biomolecules undergo to converge upon the often-altered forms we detect as fossil biomolecules. Past ecological interactions might even be chemically detected in fossil plants and their fossil herbivorous consumers, if specific biomolecules can be detected in both.

Many organic plant fossils with interesting modern relatives have been and could be further analyzed with mass spectrometry to hunt for peculiar fossilized secondary metabolites with preservation potential (Fig. 6) or their diagenetic products (e.g., hydrocarbon skeletons, ideally still diagnostic to the parent molecule). Candidate fossil biomolecules could even comprise terpenoid-related (like in copal/amber) and other molecules with low aqueous solubility, limiting their potential loss into sediment pore waters. Though, the volatility of some

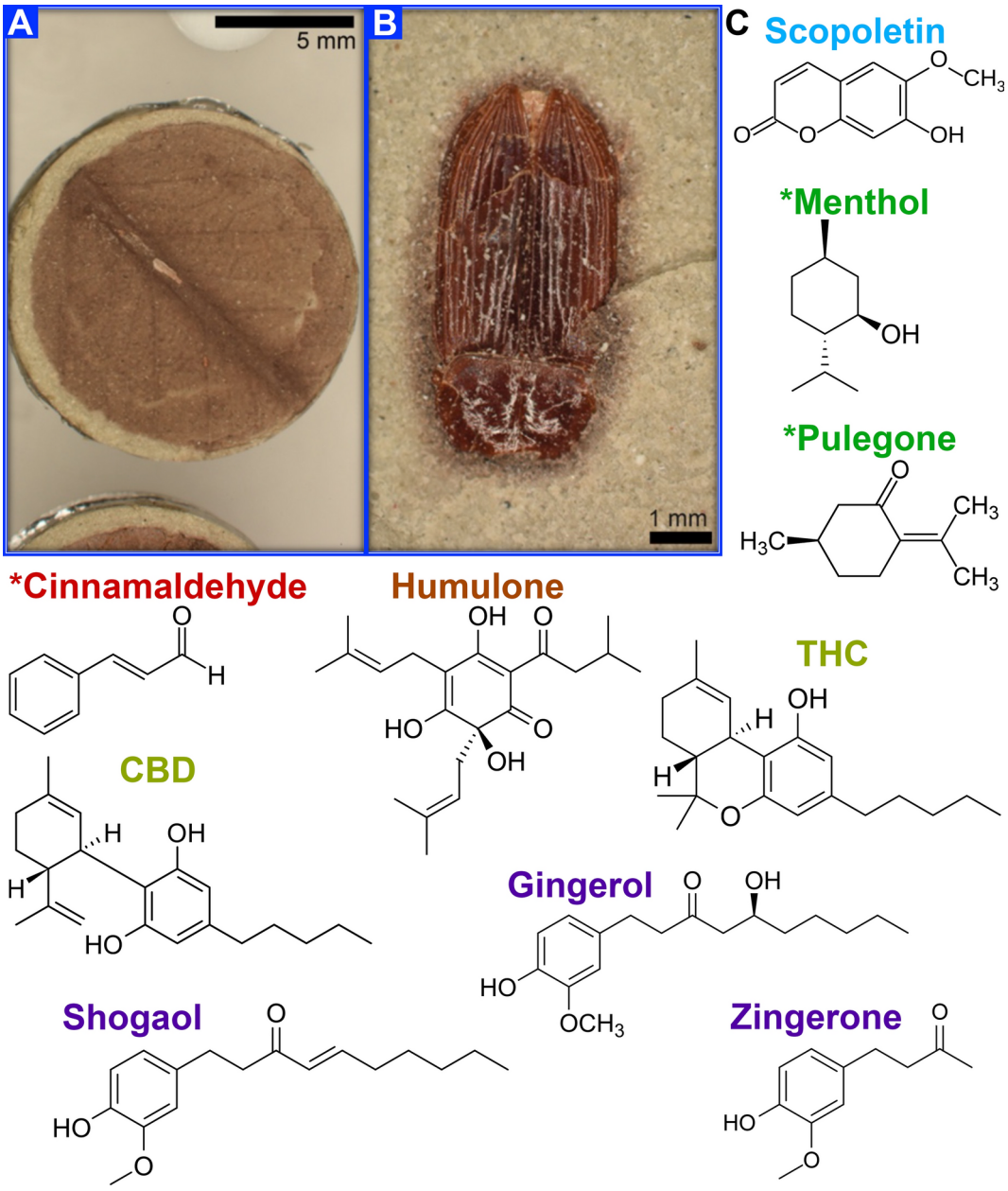

Fig. 6. Formulating intriguing hypotheses for candidate plant secondary metabolites to search for in the fossil record. Their diagenesis could be studied experimentally using sediment-encased maturation. In addition to resin maturation here, our method has already shown success at simulating carbonaceous compression fossils – whereby carbohydrate-based (**A**) plant tissues such as leaves (i.e., cellulose) and (**B**) arthropod cuticles (i.e., chitin) survive well through experimental maturation as compressed, darkened, organic residues (modified from Saitta et al.[25]), as they do through natural diagenesis. (**C**) Candidate fossil biomolecules with predicted high diagenetic thermodynamic stability: *Humulus* humulone, *Cinnamomum* *cinnamaldehyde, *Cannabis* THC and CBD, Lamiaceae (e.g., *Mentha*) *pulegone and *menthol, Zingiberaceae gingerol, zingerone, and shogaol, and Platanaceae scopoletin. *However, structures with the highest predicted volatility may be less likely to preserve well in fossils, unless contained by or incorporated into their surrounding matrix. All chemical structures are from public domain Wikimedia Commons.

compounds (e.g., odor/flavor compounds) might require sufficient retention from or direct incorporation into (i.e., bonding) the structural biopolymer components of plant fossils (e.g., lignin, cellulose) or the supramolecular structure of ancient resins. Some candidate taxa for fossil biomolecules that could first be studied using taphonomic experiments might include the following (especially if the compound is thermodynamically stable but potentially volatile, unless trapped within a matrix or capable of polymerizing/cross-linking with other molecules):

1) Eocene *Humulus* fossils[134] whose modern forms produce the isoprenoid-bearing humulone (i.e., bitter hops flavor in beer)[135]
2) Rare Cenozoic *Cannabis* fossils[136] whose modern forms produce cannabinoids that are biosynthesized from terpenes[137], such as the medicinal cannabidiol (CBD)[138] and the psychoactive, aromatic tetrahydrocannabinol (THC)[139]
3) Cretaceous *Cinnamomum* fossils[140] whose modern forms produce cinnamaldehyde (i.e., cinnamon flavor) that possesses a stable aromatic ring[141], although the volatility of this molecule might pose a challenge for retention in fossils
4) Pliocene fossil *Mentha* from the mint family (Lamiaceae)[142] whose modern forms produce the monoterpene pulegone (i.e., peppermint odor) as well as mintlactone (i.e., minty odor) and the simple monoterpenoid menthol[143], although the volatility of these molecules might limit their retention in fossils
5) Fossil Zingiberaceae (ginger family) as old as the Late Cretaceous[144] whose modern forms produce the phenolic gingerol (i.e., ginger flavor), which possesses a stable aromatic ring and can be altered through heat or desiccation into the related compounds, zingerone (a compound similar to vanillin) and shogaol[145] – thus representing possible diagenetic products of gingerol that might also be produced in experimental maturation
6) Eocene fossil Platanaceae (sycamore family)[146] whose modern forms produce the antimicrobial/antiparasitic coumarin scopoletin[147], which contains a stable aromatic ring.

Even in cases where a specific molecule that imparts a particular function or flavor is not unique to a plant taxon, interesting organic compositional profiles might still be detected in fossils. For example, cacoa is predicted through molecular phylogenies to have diverged about 10 Ma[148]. Chocolate flavor that humans sense ultimately comes from a suite of compounds, some of which are volatile, rather than a specific molecule[149]. Based on their predicted thermodynamic stability alone, many of these compounds might have some preservation potential (e.g., aromatic polyphenols, volatile heterocyclic aromatic pyrazines[150]). Could the more stable components of an organically preserved fossil *Theobroma* tree (e.g., structural biopolymers such as lignin, carbohydrates such as cellulose, kerogens derived from in situ polymerization of aliphatic lipids such as leaf waxes, or ancient resins) trap or even directly incorporate (i.e., bond to) the more volatile compounds? If so, then a suite of compounds involved in chocolate flavor might be detected when compared to taphonomic experiments and analyzed alongside appropriate controls (e.g., surrounding sediment, other plant fossils from the same formation, modern relatives of those plant taxa).

Again, these are hypotheses that should now be easier to test, given the broad utility of sediment-encased maturation at simulating disparate modes of plant tissue fossilization (i.e., carbonaceous compression fossils and ancient resins). Experimental taphonomy opens the door for paleontology to become a more predictive science than it has historically been, whereby experiments guide the hunt for previously undetected fossil biomolecules that would inform upon paleo-physiology and paleo-ecology.

Conclusion

Sediment-encased maturation was previously shown to reasonably approximate key aspects of the diagenesis of carbonaceous compression fossils from the macroscopic to the chemical level[25,26]. Here we show that sediment-encased maturation can also alter modern resins into substances that resemble natural copal and amber across a variety of material and optical properties, as well as chemical composition. Our results suggest that volatile/labile compound loss into the sediment matrix occurred in our matured resins, as in sub-fossil copal. It is also possible that polymerization/cross-linking and some aromatization occurred in our matured resins, as in fossil amber. These results represent a proof-of-concept for the use of sediment-encased maturation to study not just the formation of fossil resins, but eventually the diagenesis of copal and amber inclusions. Future work should refine the precise temperature and pressure regimes, as well as the source species (e.g., resins from Cupressaceae and Araucariaceae more amenable to polymerization/cross-linking), needed to more closely approximate fossil resins.

The availability of such an experimental approach to study the diagenesis of diverse plant tissues, whether carbonaceous compression fossils or fossil resins, would hone our search for fossil biomolecules. The future discovery of fossil plant secondary metabolites (whose volatility might be counteracted by retention from organic matrices, such as lignin or resins), guided by sediment-encased maturation of plant structural tissues, resins, and insects, could provide novel insights into paleobiology (e.g., plant and herbivore ecological interactions).

Data availability

All data generated or analysed during this study are included in this published article [and its supplementary information files].

Received: 9 October 2024; Accepted: 5 February 2025
Published online: 24 March 2025

References

1. Parry, L. A. et al. Soft-bodied fossils are not simply rotten carcasses–toward a holistic understanding of exceptional fossil preservation: Exceptional fossil preservation is complex and involves the interplay of numerous biological and geological processes. *BioEssays* **40**(1), 1700167 (2018).
2. Briggs, D. E. & McMahon, S. The role of experiments in investigating the taphonomy of exceptional preservation. *Palaeontology* **59**(1), 1–11 (2016).

3. Rhead, M. M., Eglinton, G. & Draffan, G. H. Hydrocarbons produced by the thermal alteration of cholesterol under conditions simulating the maturation of sediments. *Chem. Geol.* **8**, 277–297 (1971).
4. Peters, K. E., Rohrback, B. G. & Kaplan, I. R. Carbon and hydrogen stable isotope variations in kerogen during laboratory-simulated thermal maturation. *Am. Assoc. Petrol. Geol. Bull.* **65**, 501–508 (1981).
5. Lewan, M. D. Effects of thermal maturation on stable organic carbon isotopes as determined by hydrous pyrolysis of Woodford Shale. *Geochim. et Cosmoch. Acta* **47**, 1471–1479 (1983).
6. Monthioux, M., Landais, P. & Monin, J. C. Comparison between natural and artificial maturation series of humic coals from the Mahakam delta, Indonesia. *Organic Geochem.* **8**, 275–292 (1985).
7. Lewan, M. D., Bjorøy, M. & Dolcater, D. L. Effects of thermal maturation on steroid hydrocarbons as determined by hydrous pyrolysis of Phosphoria Retort Shale. *Geochim.et Cosmochim. Acta* **50**, 1977–1987 (1986).
8. Rullkötter, J. & Marzi, R. Natural and artificial maturation of biological markers in a Toarcian shale from northern Germany. *Organic Geochem.* **13**, 639–645 (1988).
9. Teerman, S. C. & Hwang, R. J. Evaluation of the liquid hydrocarbon potential of coal by artificial maturation techniques. *Organic Geochem.* **17**, 749–764 (1991).
10. Behar, F. et al. Experimental simulation of gas generation from coals and a marine kerogen. *Chem. Geol.* **126**, 247–260 (1995).
11. Behar, F., Tang, Y. & Liu, J. Comparison of rate constants for some molecular tracers generated during artificial maturation of kerogens: Influence of kerogen type. *Organic Geochem.* **26**, 281–287 (1997).
12. Behar, F., Lewan, M. D., Lorant, F. & Vandenbroucke, M. Comparison of artificial maturation of lignite in hydrous and nonhydrous conditions. *Organic Geochem.* **34**, 575–600 (2003).
13. Koopmans, M. P., De Leeuw, J. W., Lewan, M. D. & Sinninghe Damste, J. S. Impact of dia- and catagenesis on sulphur and oxygen sequestration of biomarkers as revealed by artificial maturation of an immature sedimentary rock. *Organic Geochem.* **25**, 391–426 (1996).
14. Stankiewicz, B. A. et al. Alternative origin of aliphatic polymer in kerogen. *Geology* **28**, 559–562 (2000).
15. Versteegh, G. J. et al. An example of oxidative polymerization of unsaturated fatty acids as a preservation pathway for dinoflagellate organic matter. *Organic Geochem.* **35**, 1129–1139 (2004).
16. Gupta, N. S., Michels, R., Briggs, D. E. G., Evershed, R. P. & Pancost, R. D. The organic preservation of fossil arthropods: An experimental study. *Proceed. Royal Soci. B* **273**, 2777–2783 (2006).
17. Gupta, N. S. et al. Experimental evidence for the formation of geomacromolecules from plant leaf lipids. *Organic Geochem.* **38**, 28–36 (2007).
18. Schimmelmann, A., Sessions, A. L. & Mastalerz, M. Hydrogen isotopic (D/H) composition of organic matter during diagenesis and thermal maturation. *Annual Rev. Earth Planet. Sci.* **34**, 501–533 (2006).
19. Schiffbauer, J. D. et al. Thermally-induced structural and chemical alteration of organic-walled microfossils: An experimental approach to understanding fossil preservation in metasediments. *Geobiology* **10**, 402–423 (2012).
20. Glass, K. et al. Impact of diagenesis and maturation on the survival of eumelanin in the fossil record. *Organic Geochem.* **64**, 29–37 (2013).
21. McNamara, M. E., Briggs, D. E. G., Orr, P. J., Field, D. J. & Wang, Z. Experimental maturation of feathers: Implications for reconstructions of fossil feather colour. *Biol. Lett.* **9**, 20130184 (2013).
22. Colleary, C. et al. Chemical, experimental, and morphological evidence for diagenetically altered melanin in exceptionally preserved fossils. *Proceed. Nat. Acad. Sci.* **112**, 12592–12597 (2015).
23. Slater, T. S. et al. Taphonomic experiments resolve controls on the preservation of melanosomes and keratinous tissues in feathers. *Palaeontology* **63**(1), 103–115 (2020).
24. Slater, T. S. et al. Taphonomic experiments reveal authentic molecular signals for fossil melanins and verify preservation of phaeomelanin in fossils. *Nat. Commun.* **14**(1), 5651 (2023).
25. Saitta, E. T., Kaye, T. G. & Vinther, J. Sediment-encased maturation: A novel method for simulating diagenesis in organic fossil preservation. *Palaeontology* **62**(1), 135–150 (2019).
26. Roy, A., Pittman, M., Kaye, T. G. & Saitta, E. T. Sediment-encased pressure–temperature maturation experiments elucidate the impact of diagenesis on melanin-based fossil color and its paleobiological implications. *Paleobiology* **49**(4), 712–732 (2023).
27. Orr, P. J., Kearns, S. L. & Briggs, D. E. Elemental mapping of exceptionally preserved 'carbonaceous compression' fossils. *Palaeogeogr., Palaeoclimatol., Palaeoecol.* **277**(1–2), 1–8 (2009).
28. Ross, A. Complete checklist of Burmese (Myanmar) amber taxa 2023. *Mesozoic* **1**, 21–57 (2024).
29. Sadowski, E. M. et al. Conservation, preparation and imaging of diverse ambers and their inclusions. *Earth-Sci. Rev.* **220**, 103653 (2021).
30. Beck, C., Wilbur, E., Meret, S., Kossove, D. & Kermani, K. The infrared spectra of amber and the identification of Baltic amber. *Archaeometry* **8**(1), 96–109 (1965).
31. Langenheim, J. H. & Beck, C. W. Infrared spectra as a means of determining botanical sources of amber. *Science* **149**(3679), 52–55 (1965).
32. Brody, R. H., Edwards, H. G. & Pollard, A. M. A study of amber and copal samples using FT-Raman spectroscopy. *Spectroch. Acta Part A: Mol. Biomol. Spectrosc.* **57**(6), 1325–1338 (2001).
33. Abduriyim, A. et al. Characterization of 'green amber'with infrared and nuclear magnetic resonance spectroscopy. *Gems Gemol.* **45**(3), 158–177 (2009).
34. Kaur, S., Stout, E., Kaur, T. & Estridg, V. Infrared spectroscopy of amber samples from the artemision excavations of 1904/1905. Anatolia antiqua. *Eski Anadolu* **20**(1), 39–43 (2012).
35. Dietz, C., Catanzariti, G., Quintero, S. & Jimeno, A. Roman amber identified as Siegburgite. *Archaeol. Anthropol. Sci.* **6**, 63–72 (2014).
36. Li, H., Wang, X. and Zhu, Y. Identification characteristics for amber and its imitation. in *5th International Conference on Information Engineering for Mechanics and Materials* (pp. 483–488). (Atlantis Press, 2015).
37. Szwedo, J. & Stroiński, A. *Who's that girl? A singular Tropiduchidae planthopper from the Eocene Baltic amber* (Fulgoromorpha, 2017).
38. Wagner-Wysiecka, E. Mid-infrared spectroscopy for characterization of Baltic amber (succinite). *Spectroch. Acta Part A: Mol. Biomol. Spectrosc.* **196**, 418–431 (2018).
39. Verkhovskaia, I. & Prokopenko, V. Raman scattering spectra of amber. in *E3S Web of Conferences* (Vol. 164, p. 14003). EDP Sciences (2020).
40. Liang, T., Zhan, Z. W. & Zou, Y. R. Molecular simulation of resin and the calculation of molecular bond energy. *ACS Omega* **6**(42), 28254–28262 (2021).
41. Musa, M., Kaye, T. G., Bieri, W. & Peretti, A. Burmese amber compared using micro-attenuated total reflection infrared spectroscopy and ultraviolet imaging. *Appl. Spectrosc.* **75**(7), 839–845 (2021).
42. Karolina, D., Maja, M. S., Magdalena, D. S. & Grażyna, Ż. Identification of treated Baltic amber by FTIR and FT-Raman–a feasibility study. *Spectrochim. Acta Part A: Mol. Biomol. Spectrosc.* **279**, 121404 (2022).
43. García-Vallès, M., Di Mariano, A., Alfonso, P., Noguès, J. & Martinez, S. Differentiation between copal and amber by their structure and thermal behaviour. *J. Thermal Anal. Calor.* **148**(23), 13027–13037 (2023).
44. Pańczak, J., Kosakowski, P. & Zakrzewski, A. Biomarkers in fossil resins and their palaeoecological significance. *Earth-Sci. Rev.* **242**, 104455 (2023).

45. Xing, L. et al. A feathered dinosaur tail with primitive plumage trapped in mid-Cretaceous amber. *Curr. Biol.* **26**(24), 3352–3360 (2016).
46. Yu, T. et al. An ammonite trapped in Burmese amber. *Proceed. Nat. Acad. Sci.* **116**(23), 11345–11350 (2019).
47. Mitchell, J. L., McKellar, R. C., Barbi, M., Coulson, I. M. & Bukejs, A. Morphological and organic spectroscopic studies of a 44-million-year-old leaf beetle (Coleoptera: Chrysomelidae) in amber with endogenous remains of chitin. *Sci. Rep.* **13**(1), 5876 (2023).
48. Beimforde, C. et al. Ectomycorrhizas from a Lower Eocene angiosperm forest. *New Phytologist* **192**, 988–996 (2011).
49. McCoy, V. E. et al. Ancient amino acids from fossil feathers in amber. *Scientific reports* **9**(1), 6420 (2019).
50. Saitta, E. T. et al. Non-avian dinosaur eggshell calcite can contain ancient, endogenous amino acids. *Geochim. et Cosmochim. Acta* **365**, 1–20 (2024).
51. DeSalle, R., Gatesy, J., Wheeler, W. & Grimaldi, D. DNA sequences from a fossil termite in Oligo-Miocene amber and their phylogenetic implications. *Science* **257**(5078), 1933–1936 (1992).
52. Austin, J. J., Ross, A. J., Smith, A. B., Fortey, R. A. & Thomas, R. H. Problems of reproducibility–does geologically ancient DNA survive in amber–preserved insects. *Proceed. Royal Soci. London Series B: Biol. Sci.* **264**(131), 467–474 (1997).
53. McCoy, V. E., Soriano, C. & Gabbott, S. E. A review of preservational variation of fossil inclusions in amber of different chemical groups. *Earth Environ. Sci. Trans. Royal Soci. Edinburgh* **107**(2–3), 203–211 (2016).
54. Labandeira, C.C. Amber. in *Reading and Writing of the Fossil Record: Preservational Pathways to Exceptional Fossilization: Presented as a Paleontological Society Short Course at the Annual Meeting of the Geological Society of America*, Vancouver, British Columbia, October 18, 2014. Paleontological Society (2014).
55. McCoy, V. E. et al. Volatile and semi-volatile composition of Cretaceous amber. *Cretac. Res.* **127**, 104958 (2021).
56. Sarria-Villa, R. A., Gallo-Corredor, J. A. & Benítez-Benítez, R. Characterization and determination of the quality of rosins and turpentines extracted from Pinus oocarpa and Pinus patula resin. *Heliyon* https://doi.org/10.1016/j.heliyon.2021.e07834 (2021).
57. Gold, D., Hazen, B. & Miller, W. G. Colloidal and polymeric nature of fossil amber. *Organic Geochem.* **30**(8), 971–983 (1999).
58. Ragazzi, E. & Schmidt, A. R. Amber. In *Encyclopedia of Geobiology, Encyclopedia of earth sciences series* (eds Reitner, J. & Thiel, V.) (Springer, Dordrecht, 2011). https://doi.org/10.1007/978-1-4020-9212-1_9.
59. Poinar, G. O., Poinar, H. N. & Cano, R. J. DNA from Amber inclusions. In *Ancient DNA* (eds Herrmann, B. & Hummel, S.) (Springer, New York NY, 1994). https://doi.org/10.1007/978-1-4612-4318-2_6.
60. Wolfe, A. P. et al. A new proposal concerning the botanical origin of Baltic amber. *Proceed. Royal Soci. B: Biol. Sci.* **276**(1672), 3403–3412 (2009).
61. Matuszewska, A. Bursztyn (sukcynit), inne żywice kopalne, subfosylne i współczesne [Amber (Succinite) and other modern, subfossil and fossil resins)]. 234 pp. (Ofcyna Wydawnicza Wacław Walasek, Katowice, 2010)
62. Zheng, T. et al. Spectroscopic identification of amber imitations: Different pressure and temperature treatments of copal resins. *Crystals* **11**(10), 1223 (2021).
63. Pastorelli, G. A comparative study by infrared spectroscopy and optical oxygen sensing to identify and quantify oxidation of Baltic amber in different ageing conditions. *J. Cult. Herit.* **12**(2), 164–168 (2011).
64. Bisulca, C., Nascimbene, P. C., Elkin, L. & Grimaldi, D. A. Variation in the deterioration of fossil resins and implications for the conservation of fossils in amber. *Am. Museum Novitat.* **2012**(3734), 1–19 (2012).
65. McCoy, V. E. et al. Unlocking preservation bias in the amber insect fossil record through experimental decay. *PLoS One* **13**(4), e0195482 (2018).
66. Favrot, A., Cohen, S.X., Schöder, S. & Gueriau, P. Assessing the potential of high-resolution synchrotron microtomography to document the preservation of insects in amber. in *4th Virtual Palaeontological Congress*, May 8th–22nd, (2023).
67. Seyfullah, L. J., Roberts, E. A., Jardine, P. E., Schmidt, B. C. & Schmidt, A. R. Experimental induction of resins as a tool to understand variability in ambers. *Fossil Record* **24**, 321–337 (2021).
68. Seyfullah, L. J., Roberts, E. A., Jardine, P. E., Rikkinen, J. & Schmidt, A. R. Uncovering the natural variability of araucariacean exudates from ex situ and in situ tree populations in New Caledonia using FTIR spectroscopy. *PeerJ Anal. Chem.* **4**, e17 (2022).
69. Hillwig, M. L., Mann, F. M. & Peters, R. J. Diterpenoid biopolymers: New directions for renewable materials engineering. *Biopolymers* **95**(2), 71–76 (2011).
70. Bouju, V. and Perrichot, V., 2020. A review of amber and copal occurrences in Africa and their paleontological significance. Bulletin de la Société Géologique de France, 191(1).
71. Sadowski, E.-M., Schmidt, A. R. & Kunzmann, L. The hyperdiverse conifer flora of the Baltic amber forest. *Palaeontograph., Abteilung B: Palaeobotany—Palaeophytology* **304**, 1–148 (2022).
72. Hall, D. E. et al. Evolution of conifer diterpene synthases: Diterpene resin acid biosynthesis in lodgepole pine and jack pine involves monofunctional and bifunctional diterpene synthases. *Plant Physiol.* **161**(2), 600–616 (2013).
73. Alicandri, E. et al. Diterpene resin acids and olefins in Calabrian pine (Pinus nigra subsp laricio (Poiret) Maire) oleoresin: GC-MS profiling of major diterpenoids in different plant organs, molecular identification and expression analysis of diterpene synthase genes. *Plants* **10**(11), 2391 (2021).
74. Spalding, B. P., Zinkel, D. F. & Roberts, D. R. New labdane resin acids from Pinus elliottii. *Phytochemistry* **10**(12), 3289–3292 (1971).
75. Zinkel, D. F., Magee, T. V. & Walter, J. Major resin acids of Pinus nigra needles. *Phytochemistry* **24**(6), 1273–1277 (1985).
76. Zinkel, D. F. & Magee, T. V. Diterpene resin acids from the needle oleoresin of Pinus strobus. *Phytochemistry* **26**(3), 769–774 (1987).
77. Jeong, S. Y. et al. Labdane-type Diterpenes from Pinus eldarica Needles and Their Anti-Helicobacter pylori Activity. *ACS omega* **7**(33), 29502–29507 (2022).
78. Anderson, K. B., Winans, R. E. & Botto, R. E. The nature and fate of natural resins in the geosphere—II. Identification, classification and nomenclature of resinites. *Organic Geochem.* **18**(6), 829–841 (1992).
79. Garneau, F. X., Collin, G., Gagnon, H. & Pichette, A. Chemical composition of the hydrosol and the essential oil of three different species of the Pinaceae family: Picea glauca (Moench) Voss Picea mariana (Mill) BSP, and Abies balsamea (L) Mill. *J Essent Oil Bear Plants* **15**(2), 227–236 (2012).
80. Poinar, G. *Life in Amber* 368 (Stanford University Press, 1992).
81. McKellar, R. C. & Wolfe, A. P. *Canadian amber. Biodiversity of fossils in amber from the major world deposits* 149–166 (Siri Scientific Press, Manchester, 2010).
82. Wolfe, A. P., McKellar, R. C., Tappert, R., Sodhi, R. N. & Muehlenbachs, K. Bitterfeld amber is not Baltic amber: Three geochemical tests and further constraints on the botanical affinities of succinite. *Rev. Palaeobot. Palynol.* **225**, 21–32 (2016).
83. Verkhovskaia, I. Baltic amber inspection: Micro-macro-structural and luminescent analysis. In E3S Web of Conferences (Vol. 138, p. 01010). EDP Sciences (2019).
84. Stilwell, J. D. et al. Amber from the Triassic to Paleogene of Australia and New Zealand as exceptional preservation of poorly known terrestrial ecosystems. *Sci. Report* **10**(1), 5703 (2020).
85. Czajkowski, M. J. Amber from the Baltic. *Mercian Geologist* **17**(2), 86 (2009).
86. Saunders, W. B., Mapes, R. H., Carpenter, F. M. & Elsik, W. C. Fossiliferous amber from the Eocene (Claiborne) of the Gulf coastal plain. *Geol. Soci. Am. Bull.* **85**(6), 979–984 (1974).
87. Xing, Q. Y., Yang, M., Yang, H. X. & Zu, E. D. Study on the gemological characteristics of amber from Myanmar and Chinese Fushun. *Key Eng. Mater.* **544**, 172–177 (2013).

88. Roghi, G., Kustatscher, E., Ragazzi, E. & Giusberti, L. Middle Triassic amber associated with Voltzialean conifers from the Southern Alps of Italy. *Rivista italiana di paleontologia e stratigrafia* **123**(2), 193–202 (2017).
89. Xing, L. et al. A gigantic marine ostracod (Crustacea: Myodocopa) trapped in mid-Cretaceous Burmese amber. *Sci. Report* **8**(1), 1365 (2018).
90. McKellar, R. C. et al. A direct association between amber and dinosaur remains provides paleoecological insights. *Sci. Report* **9**(1), 17916 (2019).
91. Clark, A. T. et al. Evaluation of fossil amber birefringence and inclusions using terahertz time-domain spectroscopy. *Polymers* **14**(24), 5506 (2022).
92. Berner, R. A. & Landis, G. P. Gas bubbles in fossil amber as possible indicators of the major gas composition of ancient air. *Science* **239**(4846), 1406–1409 (1988).
93. Hopfenberg, H. B., Witchey, L. C. & Poinar, G. O. Jr. Is the air in amber ancient?. *Science* **241**(4866), 717–718 (1988).
94. Horibe, Y. & Craig, H. Is the air in amber ancient?. *Science* **241**(4866), 720–721 (1988).
95. Landis, G. P. & Berner, R. A. Analysis of gases in fossil amber. *Am J. Sci.* **318**(5), 590–601 (2018).
96. Cunningham, A., Gay, I. D., Oehlschlager, A. C. & Langenheim, J. H. 13C NMR and IR analyses of structure, aging and botanical origin of Dominican and Mexican ambers. *Phytochemistry* **22**(4), 965–968 (1983).
97. Langenheim, J.H. Plant resins: Chemistry, evolution, ecology, and ethnobotany. (No Title) (2003).
98. Kong, D., Meng, Y. & McKenna, G. B. Determination of the molecular weight between cross-links for different ambers: Viscoelastic measurements of the rubbery plateau. *Polymer Eng. Sci.* **62**(4), 1023–1040 (2022).
99. Anderson, K. B. & Crelling, J. C. Introduction. In Amber, Resinite and Fossil Resins (eds K. B. Anderson and J. C. Crelling), pp. xi–xvii. American Chemical Society, Washington D. C (1995).
100. Anderson, K. B. & Botto, R. E. The nature and fate of natural resins in the geosphere—III. Re-evaluation of the structure and composition of Highgate Copalite and Glessite. *Organic Geochem.* **20**(7), 1027–1038 (1993).
101. Anderson, K. B. Resin and amber in sediments. In *Sedimentology. Encyclopedia of Earth Science* (Springer, Berlin and Heidelberg, 1978). https://doi.org/10.1007/3-540-31079-7_171.
102. Llevot, A., Grau, E., Carlotti, S., Grelier, S. & Cramail, H. Dimerization of abietic acid for the design of renewable polymers by ADMET. *Eur. Polymer J.* **67**, 409–417 (2015).
103. Zheng, H. et al. Enhanced conversion of rosin to polymerized rosin with reusable Brønsted acid deep eutectic solvent. *Ind. Crops Prod.* **221**, 119414 (2024).
104. Nerg, A. et al. Seasonal and geographical variation of terpenes, resin acids and total phenolics in nursery grown seedlings of Scots pine (*Pinus sylvestris* L.). *New Phytol.* **128**(4), 703–713 (1994).
105. Skakovskii, E. D., Yu, L., Gapankova, E. I., Popoff, E. H. & Lamotkin, S. A. Seasonal changes in the composition of scots pine (*Pinus Syvestris* L.) oleoresin, measured by the NMR method. *Russ. J. Bioorgan. Chem.* **49**(7), 1658–1666 (2023).
106. Ilek, A., Gąsecka, M., Magdziak, Z., Saitanis, C. & Siegert, C. M. Seasonality affects low-molecular-weight organic acids and phenolic compounds' composition in scots pine litterfall. *Plants* **13**(10), 1293 (2024).
107. Wallis, C. et al. Differential effects of nutrient availability on the secondary metabolism of Austrian pine (Pinus nigra) phloem and resistance to Diplodia pinea. *Forest Pathol.* **41**(1), 52–58 (2011).
108. Raldugin, V. A., Hang, V. A., Dubovenko, Z. V. & Pentegova, V. A. Terpenoids of the oleoresin of Pinus pumila. *Chem. Nat. Compd.* **12**, 266–269 (1976).
109. Shpatov, A. V. et al. Composition and bioactivity of lipophilic metabolites from needles and twigs of Korean and Siberian pines (Pinus koraiensis Siebold & Zucc and Pinus sibirica Du Tour). *Chem. Biodiver.* **14**(2), 1600203 (2017).
110. Poulin, J. & Helwig, K. Inside amber: New insights into the macromolecular structure of Class Ib resinite. *Organic Geochem.* **86**, 94–106 (2015).
111. Zinkel, D. F. & Clarke, W. B. Resin acids of Pinus resinosa needles. *Phytochemistry* **24**(6), 1267–1271 (1985).
112. Zinkel, D. F., Toda, J. K. & Rowe, J. W. Occurrence of anticopalic acid in Pinus monticola. *Phytochemistry* **10**(5), 1161–1163 (1971).
113. Yang, N. Y., Liu, L., Tao, W. W., Duan, J. A. & Tian, L. J. Diterpenoids from Pinus massoniana resin and their cytotoxicity against A431 and A549 cells. *Phytochemistry* **71**(13), 1528–1533 (2010).
114. Zinkel, D. F. & Magee, T. V. Resin acids of Pinus ponderosa needles. *Phytochemistry* **30**(3), 845–848 (1991).
115. Raldugin, V. A., Demenkova, L. I. & Pentegova, V. A. New diterpenoid components of the oleoresin of Pinus pumila. *Chem. Nat. Compd.* **14**, 286–289 (1978).
116. Shpatov, A. V. et al. Lipophilic metabolites from five-needle pines, Pinus armandii and Pinus kwangtungensis, exhibiting antibacterial activity. *Chem. Biodivers.* **17**(8), e2000201 (2020).
117. de Simón, B. F., Vallejo, M. C. G., Cadahía, E., Miguel, C. A. & Martinez, M. C. Analysis of lipophilic compounds in needles of Pinus pinea L.. *Ann. Forest Sci.* **58**(4), 449–454 (2001).
118. Mei, L. et al. Identification of the diterpenoid biosynthesis genes and their expression status in relation to oleoresin yield of masson pine. *Ind. Crops Prod.* **170**, 113827 (2021).
119. Mateus, E.M.H.P. Characterization of Pinus spp. needles by gas chromatography and mass spectrometry: Application to plant-insect interactions (Doctoral dissertation, Universidade NOVA de Lisboa (Portugal)) (2008).
120. Shpatov, A. V. et al. Low-volatile lipophilic compounds in needles, defoliated twigs, and outer bark of Pinus thunbergii. *Nat. Prod. Commun.* **8**(12), 1934578X1300801227 (2013).
121. Barrero, A. F., Herrador, M. M., Arteaga, P., Arteaga, J. F. & Arteaga, A. F. Communic acids: Occurrence, properties and use as chirons for the synthesis of bioactive compounds. *Molecules* **17**(2), 1448–1467 (2012).
122. Montoro, Ó. R., Lobato, Á., Baonza, V. G. & Taravillo, M. Infrared spectroscopic study of the formation of fossil resin analogs with temperature using trans-communic acid as precursor. *Microchem. J.* **141**, 294–300 (2018).
123. Otto, A. & Wilde, V. Sesqui-, di-, and triterpenoids as chemosystematic markers in extant conifers—A review. *Botan. Rev.* **67**, 141–238 (2001).
124. Venditti, A. et al. Secondary metabolites from Pinus mugo Turra subsp mugo growing in the Majella National Park (central Apennines, Italy). *Chem. Biodiver.* **10**(11), 2091–2100 (2013).
125. Allenspach, M., Valder, C., Flamm, D., Grisoni, F. & Steuer, C. Verification of chromatographic profile of primary essential oil of *Pinus sylvestris* L. combined with chemometric analysis. *Molecules* **25**(13), 2973 (2020).
126. Helfenstein, A. et al. Antibacterial profiling of abietane-type diterpenoids. *Bioorgan. Med. Chem.* **25**(1), 132–137 (2017).
127. González, M. A. Aromatic abietane diterpenoids: Total syntheses and synthetic studies. *Tetrahedron* **71**(13), 1883–1908 (2015).
128. Sanger, J. E. Fossil pigments in paleoecology and paleolimnology. *Palaeogeogr., Palaeoclimatol., Palaeoecol.* **62**(1–4), 343–359 (1988).
129. Bliedtner, M. et al. Age and origin of leaf wax n-alkanes in fluvial sediment–paleosol sequences and implications for paleoenvironmental reconstructions. *Hydrol. Earth Syst. Sci.* **24**(4), 2105–2120 (2020).
130. Mycke, B. & Michaelis, W. Lignin-derived molecular fossils from geological materials. *Naturwissenschaften* **73**(12), 731–734 (1986).
131. Kariñho-Betancourt, E. Plant-herbivore interactions and secondary metabolites of plants: Ecological and evolutionary perspectives. *Botan. Sci.* **96**(1), 35–51 (2018).
132. Kumar, S., Saini, R., Suthar, P., Kumar, V. & Sharma, R. Plant secondary metabolites: Their food and therapeutic importance. In *Plant secondary metabolites: Physico-chemical properties and therapeutic applications* 371–413 (Springer Nature, Singapore, 2022).

133. Peris, D. & Rust, J. Cretaceous beetles (Insecta: Coleoptera) in amber: The palaeoecology of this most diverse group of insects. *Zool. J. Linnean Soci.* **189**(4), 1085–1104 (2020).
134. Tihelka, E., Wang, Y., Cai, C., Small, E., McPartland, J. M. The deep evolutionary roots of Cannabis and Humulus: Fossils, genomics, and geography", Mendeley Data, V3, https://doi.org/10.17632/4fzdts2nj6.3 (2022)
135. Urban, J., Dahlberg, C. J., Carroll, B. J. & Kaminsky, W. Absolute configuration of beer's bitter compounds. *Angewandte Chemie (International ed. in English)* **52**(5), 1553 (2013).
136. McPartland, J. M. Cannabis systematics at the levels of family, genus, and species. *Cannabis Cannabinoid Res.* **3**(1), 203–212 (2018).
137. Sommano, S. R., Chittasupho, C., Ruksiriwanich, W. & Jantrawut, P. The cannabis terpenes. *Molecules* **25**(24), 5792 (2020).
138. Campos, A. C., Moreira, F. A., Gomes, F. V., Del Bel, E. A. & Guimaraes, F. S. Multiple mechanisms involved in the large-spectrum therapeutic potential of cannabidiol in psychiatric disorders. *Philosoph. Trans. Royal Soci. B: Biol. Sci.* **367**(1607), 3364–3378 (2012).
139. Gaoni, Y. & Mechoulam, R. Isolation, structure, and partial synthesis of an active constituent of hashish. *J. Am. Chem. Soci.* **86**(8), 1646–1647 (1964).
140. Huang, J. F. et al. Origins and evolution of cinnamon and camphor: A phylogenetic and historical biogeographical analysis of the Cinnamomum group (Lauraceae). *Mol. Phylogenet. Evol.* **96**, 33–44 (2016).
141. Gutzeit, H. & Ludwig-Müller, J. *Plant natural products: Synthesis, Biological functions and practical applications* 19–21 (Wiley, 2014).
142. Velichkevich, F. Y. & Zastawniak, E. The Pliocene flora of Kholmech, south-eastern Belarus and its correlation with other Pliocene floras of Europe. *Acta Palaeobot.* **43**(2), 137–259 (2003).
143. El Omari, N. et al. GC-MS-MS analysis and biological properties determination of Mentha piperita L., essential oils. *Biochem. Systemat. Ecol.* **116**, 104875 (2024).
144. Smith, S. Y., Iles, W. J., Benedict, J. C. & Specht, C. D. Building the monocot tree of death: Progress and challenges emerging from the macrofossil-rich Zingiberales. *Am. J. Botany* **105**(8), 1389–1400 (2018).
145. Connell, D. W. & Sutherland, M. D. A re-examination of gingerol, shogaol, and zingerone, the pungent principles of ginger (Zingiber officinale Roscoe). *Austral. J. Chem.* **22**(5), 1033–1043 (1969).
146. Manchester, S. R. Fossil plants of the Eocene Clarno nut beds. *Oregon Geol.* **43**(6), 75–81 (1981).
147. Tanaka, Y., Data, E. S., Hirose, S., Taniguchi, T. & Uritani, I. Biochemical changes in secondary metabolites in wounded and deteriorated cassava roots. *Agricult. Biol. Chem.* **47**(4), 693–700 (1983).
148. Richardson, J. E., Whitlock, B. A., Meerow, A. W. & Madriñán, S. The age of chocolate: A diversification history of Theobroma and Malvaceae. *Front. Ecol. Evolut.* **3**, 120 (2015).
149. Aprotosoaie, A. C., Luca, S. V. & Miron, A. Flavor chemistry of cocoa and cocoa products—An overview. *Comprehens. Rev. Food Sci. Food Safety* **15**(1), 73–91 (2016).
150. Saitta, E. T. et al. Low fossilization potential of keratin protein revealed by experimental taphonomy. *Palaeontology* **60**(4), 547–556 (2017).

Acknowledgements

We thank two anonymous reviewers for their very helpful feedback. We thank Jess Goehler (Chicago Botanic Garden) for assistance in collecting resin samples and Akiko Shinya (Field Museum of Natural History) for preparing one of the synthetic resin samples (Run B dry *P. sylvestris*). We also thank Friedrich Menges (Spectroscopy Ninja) for clarification on Spectragryph software. Jakob Vinther (University of Bristol) assisted with the original study of sediment-encased maturation, from which Figs. 4, 6A–B were derived [25]. Finally, we thank the Paul Sereno (University of Chicago) Fossil Lab for housing the sediment-encased maturation equipment. Fig. 5B is modified from the December 2017 Palaeontology Association copyright in Szwedo & Stroiński [37] under the terms of Creative Commons Attribution-NonCommercial-ShareAlike 4.0 International (CC BY-NC-SA 4.0). All molecular structures in Fig. 6 come from public domain Wikimedia Commons.

Author contributions

Both E.T.S. and T.G.K. designed and performed experiments and contributed to writing.

Declarations

Competing interests

The authors declare no competing interests.

Additional information

Supplementary Information The online version contains supplementary material available at https://doi.org/10.1038/s41598-025-89448-5.

Correspondence and requests for materials should be addressed to E.T.S.